Acta Cryst E
CRYSTALLOGRAPHIC COMMUNICATIONS
ISSN 2056-9890

Crystal structure and Hirshfeld surface analysis of supramolecular aggregate of 2,2,6,6-tetramethylpiperidin-1-ium bromide with 1,2,3,4-tetrafluoro-5,6-diiodobenzene

Atash V. Gurbanov,[a,b,c] Tuncer Hökelek,[d] Gunay Z. Mammadova,[e] Khudayar I. Hasanov,[f,g] Tahir A. Javadzade[h] and Alebel N. Belay[i]*

[a]Excellence Center, Baku State University, Z. Xalilov Str. 23, AZ 1148 Baku, Azerbaijan, [b]Scientific Research Center, Baku Engineering University, Hasan Aliyev Str. 120, Baku, Absheron AZ0101, Azerbaijan, [c]Centro de Quimica Estrutural, Instituto Superior Tecnico, Universidade de Lisboa, Av. Rovisco Pais, 1049-001 Lisbon, Portugal, [d]Hacettepe University, Department of Physics, 06800 Beytepe-Ankara, Türkiye, [e]Department of Chemistry, Baku State University, Z. Khalilov Str. 23, Az 1148 Baku, Azerbaijan, [f]Western Caspian University, Istiglaliyyat Str. 31, AZ 1001 Baku, Azerbaijan, [g]Azerbaijan Medical University, Scientific Research Centre (SRC), A. Kasumzade Str. 14, AZ 1022 Baku, Azerbaijan, [h]Department of Chemistry and Chemical Engineering, Khazar University, Mahzati Str. 41, AZ 1096 Baku, Azerbaijan, and [i]Department of Chemistry, Bahir Dar University, PO Box 79, Bahir Dar, Ethiopia. *Correspondence e-mail: alebel.nibret@bdu.edu.et

Received 29 October 2024
Accepted 26 November 2024

Edited by C. Schulzke, Universität Greifswald, Germany

Keywords: crystal structure; non-covalent interactions; halogen bond.

Supporting information: this article has supporting information at journals.iucr.org/e

The asymmetric unit of the title compound, $C_9H_{20}N^+{\cdot}Br^-{\cdot}C_6F_4I_2$, contains one 2,2,6,6 tetramethylpiperidine-1-ium cation, one 1,2,3,4-tetrafluoro-5,6-diiodobenzene molecule, and one uncoordinated bromide anion. In the crystal, the bromide anions link the 2,2,6,6-tetramethylpiperidine molecules by intermolecular C—H···Br and N—H···Br hydrogen bonds, leading to dimers, with the coplanar 1,2,3,4-tetrafluoro-5,6-diiodobenzene molecules filling the space between them. There is a π–π interaction between the almost parallel benzene rings [dihedral angle = 10.5 (2)°] with a centroid-to-centroid distance of 3.838 (3) Å and slippage of 1.468 Å. No C—H···π(ring) interactions are observed. A Hirshfeld surface analysis indicates that the most important contributions for the crystal packing are from H···F/F···H (23.8%), H···H (22.6%), H···Br/Br···H (17.3%) and H···I/I···H (13.8%) interactions. Hydrogen bonding and van der Waals interactions are the dominant interactions in the crystal packing.

1. Chemical context

The halogen bond (HaB) is defined as a non-covalent interaction between the electron-density-deficient region (so-called σ or π hole) of a covalently bonded halogen atom and a nucleophilic (Nu) site in the same (intramolecular) or another (intermolecular) molecular entity: R—Ha···Nu [Ha = F, Cl, Br or I; R = C, Pn (pnictogen), Ch (chalcogen), metal *etc.*; Nu = lone pair possessing Ha, Ch, Pn or metal atom, π-system, anion, radical, *etc.*; Cavallo *et al.*, 2016]. Similarly to hydrogen and chalcogen bonds (Gurbanov *et al.*, 2020; Mahmudov & Pombeiro, 2016), halogen bonds can also be classified into normal halogen bonds, positive charge-assisted halogen bonds, negative charge-assisted halogen bonds and charge-assisted halogen bonds (Peuronen *et al.*, 2023). Both the strength and directionality of charge-assisted halogen bonds are much larger than those of normal halogen bonds (Gomila & Frontera, 2020; Shixaliyev *et al.*, 2014), which are traditionally regarded as favourable synthetic tools for building new supramolecular systems (Mahmoudi *et al.*, 2017*a*,*b*). In addition to their catalytic functions (Ma *et al.*, 2021), *N*-oxide radicals can act as halogen-bond acceptors (Pang *et al.*, 2013). In the context of this work, we investigated a new negative

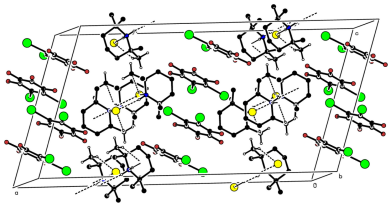

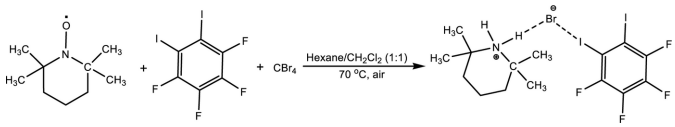

Figure 1
Synthesis of 2,2,6,6-tetramethylpiperidin-1-ium bromide from 1,2,3,4-tetrafluoro-5,6-diiodobenzene.

charge-assisted halogen-bonded supramolecular aggregate, which was obtained by the reaction of 2,2,6,6-tetramethylpiperidinyl-1-oxy (TEMPO) with 1,2,3,4-tetrafluoro-5,6- diiodobenzene in the presence of CBr_4 in a mixture of hexane/CH_2Cl_2 at 343 K (see Fig. 1). We provide herein a detailed description of the synthesis and an examination of the molecular and crystal structures together with a Hirshfeld surface analysis of the title compound, (I).

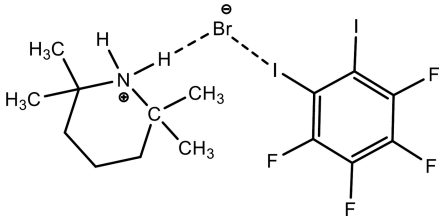

2. Structural commentary

Two molecules are present in the asymmetric unit of the title compound, 2,2,6,6-tetramethyl piperidine-1-ium and 1,2,3,4-tetrafluoro-5,6-diiodobenzene, in addition to one uncoordinated bromide ion (Fig. 2). Atoms I1, I2, F1, F2, F3 and F4 are −0.0116 (3), −0.0287 (3), 0.005 (3), −0.022 (3), −0.003 (3) and 0.033 (3) Å, respectively, away from the best least-squares plane of the benzene ring (C1–C6). All atoms of the benzene derivative are essentially coplanar. The piperidine ring (N1/C7–C11), is in a chair conformation. There are no apparent unusual bond distances or interbond angles within the two molecules.

3. Supramolecular features

With regard to intermolecular contacts, the uncoordinated bromide ions link the 2,2,6,6-tetramethylpiperidine molecules through intermolecular C—H···Br and N—H···Br hydrogen bonds (Table 1) with a double or triple acceptor atom, resulting in dimers (Fig. 3). In the crystal, the dimers are stacked along the *b*-axis direction, while the coplanar 1,2,3,4-tetrafluoro-5,6-diiodobenzene molecules protrude along the *c*-axis direction, filling the space between the dimers (Fig. 4). There is a π–π interaction between the C1–C6 benzene rings with a centroid-to-centroid distance of 3.838 (3) Å, where the dihedral angle between the benzene rings is 10.5 (2)° with a slippage of 1.468 Å.

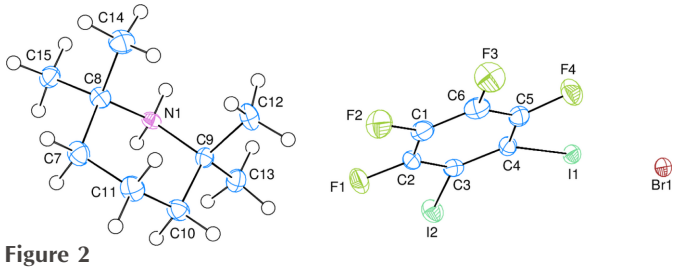

Figure 2
The title compound with atom-numbering scheme and 50% probability ellipsoids.

Table 1
Hydrogen-bond geometry (Å, °).

D—H···A	D—H	H···A	D···A	D—H···A
N1—H1A···Br1^{ii}	0.86 (2)	2.55 (2)	3.407 (3)	179 (4)
N1—H1B···Br1^{iii}	0.85 (2)	2.56 (2)	3.387 (3)	165 (5)
C13—H13C···Br1^{ii}	0.98	2.91	3.767 (4)	147

Symmetry codes: (ii) $x-\frac{1}{2}, -y+\frac{1}{2}, z-\frac{1}{2}$; (iii) $-x+1, y, -z+\frac{3}{2}$.

4. Hirshfeld surface analysis

In order to visualize the intermolecular interactions in the crystal of the title compound (I), a Hirshfeld surface (HS)

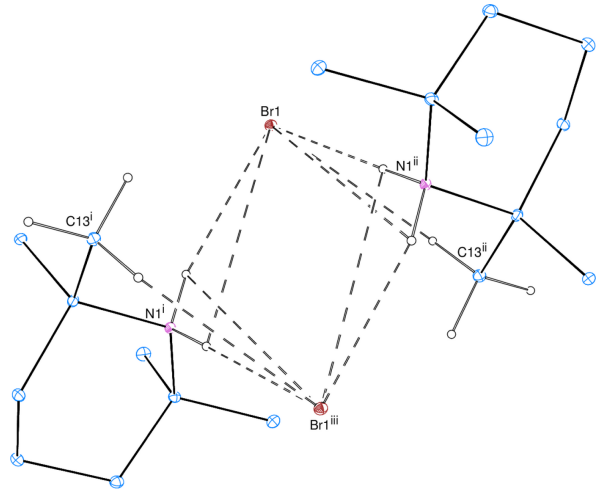

Figure 3
The H···Br contacts leading to dimerization. Intermolecular C—H···Br and N—H···Br hydrogen bonds are shown as dashed lines. H atoms not involved in these interactions are omitted for clarity.

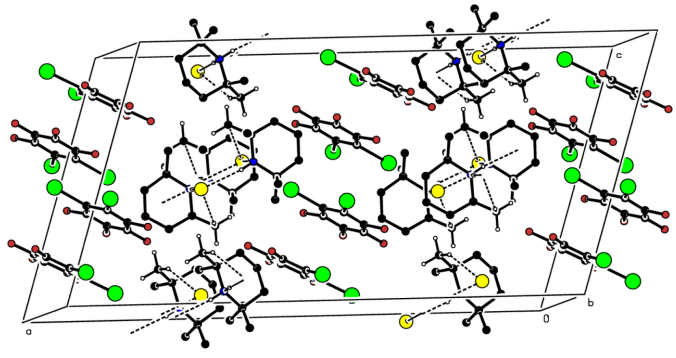

Figure 4
A partial packing diagram, viewed down the *b*-axis direction. Intermolecular C—H···Br and N—H···Br hydrogen bonds are shown as dashed lines. H atoms not involved in these interactions are omitted for clarity.

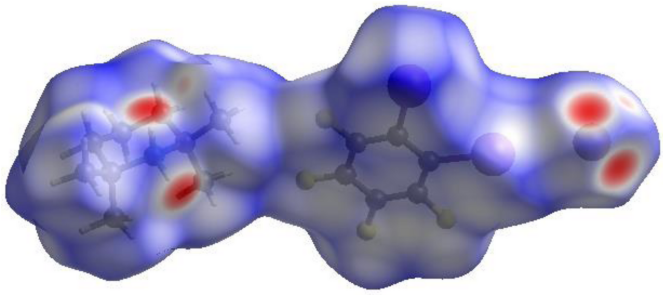

Figure 5
View of the three-dimensional Hirshfeld surface of the title compound plotted over d_{norm}.

analysis (Hirshfeld, 1977; Spackman & Jayatilaka, 2009) was carried out using *Crystal Explorer 17.5* (Spackman *et al.*, 2021). The contact distances d_i and d_e from the Hirshfeld surface to the nearest atom inside and outside, respectively, enable the analysis of the intermolecular interactions through the mapping of d_{norm}. The combination of d_i and d_e in the form of two-dimensional fingerprint plots (McKinnon *et al.*, 2004) provides a summary of intermolecular contacts in the crystal. In the HS plotted over d_{norm} (Fig. 5), the white surface indicates contacts with distances equal to the sum of van der Waals radii, and the red and blue colours indicate distances shorter (in close contact) or longer (no/weak contact) than the van der Waals radii, respectively (Venkatesan *et al.*, 2016). The bright-red spots are indicative of their roles as the respective donors and/or acceptors. The shape-index would represent any C—H···π interaction as red depressions located at the π-ring system and a blue region surrounding the respective C—H moiety, and hence Fig. 6 clearly suggests that there are no such C—H···π interactions present in (I). The shape-index of the HS can also indicate π–π stacking interactions by the presence of adjacent red and blue triangles. Fig. 6 suggests π–π interactions are present in (I).

The overall two-dimensional fingerprint plot is shown in Fig. 7*a* and those delineated into H···F/F···H, H···H, H···Br/Br···H, H···I/I···H, F···I/I···F, C···I/I···C, C···C, F···F, H···C/C···H, I···I and F···Br/Br···F contacts (McKinnon *et al.*, 2007) are illustrated in Fig. 7*b*–*l*, respectively, together with their relative contributions to the Hirshfeld surface. The most important interaction clearly is of the

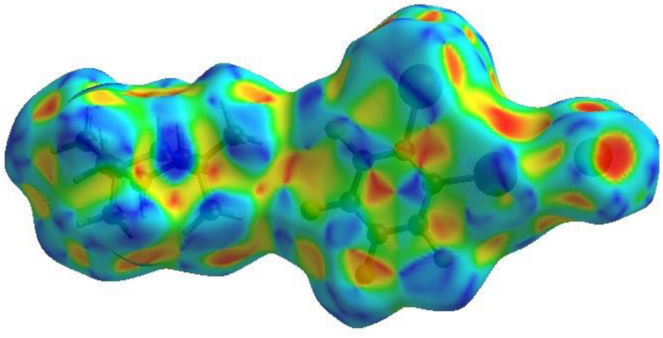

Figure 6
Hirshfeld surface of the title compound plotted over shape-index.

Table 2
Selected interatomic distances (Å).

I1···F4	3.138 (3)	C11···H14*B*	2.83
I1···I2	3.7118 (4)	C12···H11*B*	2.83
I2···F1	3.111 (3)	C12···H14*B*	2.67
I1···H15*C*^{i}	3.16	C14···H12*B*	2.72
H1*A*···Br1^{ii}	2.546 (19)	C14···H11*B*	2.90
H13*C*···Br1^{ii}	2.91	H1*A*···H13*C*	2.21
H1*B*···Br1^{iii}	2.56 (2)	H1*A*···H15*C*	2.30
F1···F2	2.670 (4)	H1*B*···H12*C*	2.19
F2···F3	2.709 (4)	H1*B*···H14*A*	2.34
F3···F4	2.654 (4)	H7*B*···H15*C*	2.40
F2···H12*A*	2.65	H11*B*···H12*B*	2.19
H11*A*···F3^{iv}	2.63	H11*B*···H14*B*	2.29
C12···C14	3.203 (6)	H12*B*···H14*B*	1.97
C11···H12*B*	2.76		

Symmetry codes: (i) $x+\frac{1}{2}, y+\frac{1}{2}, z$; (ii) $x-\frac{1}{2}, -y+\frac{1}{2}, z-\frac{1}{2}$; (iii) $-x+1, y, -z+\frac{3}{2}$; (iv) $-x+\frac{1}{2}, y-\frac{1}{2}, -z+\frac{3}{2}$.

H···F/F···H type (Table 2), contributing 23.8% to the overall crystal packing, which is reflected in Fig. 7*b* as pair of spikes with tips at $d_e + d_i = 2.52$ Å. The H···H interactions (Fig. 7*c*) contribute 22.6% to the HS and form a single maximum extension at $d_e = d_i = 1.18$ Å. The H···Br/Br···H (Fig. 7*d*) and H···I/I···H (Fig. 7*e*) contacts contribute 17.3% and 13.8%, respectively, to the HS, appearing as pairs of spikes with the

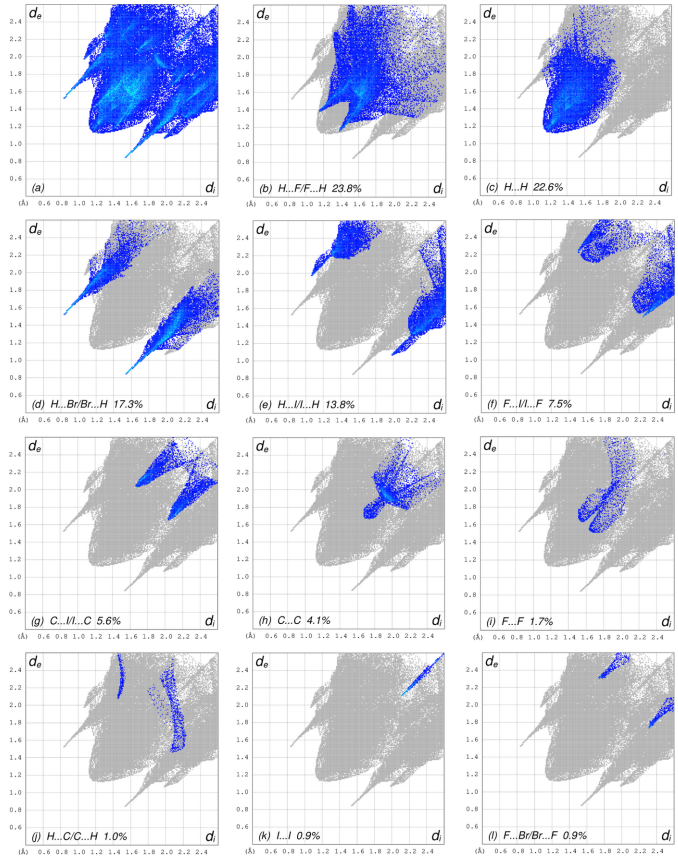

Figure 7
The full two-dimensional fingerprint plots for the title compound, showing (*a*) all interactions, and delineated into (*b*) H···F/F···H, (*c*) H···H, (*d*) H···Br/Br···H, (*e*) H···I/ ···H, (*f*) F···I/I···F, (*g*) C···I/I···C, (*h*) C···C, (*i*) F···F, (*j*) H···C/C···H, (*k*) I···I, and (*l*) F···Br/Br···F interactions. The d_i and d_e values are the closest internal and external distances (in Å) from given points on the Hirshfeld surface.

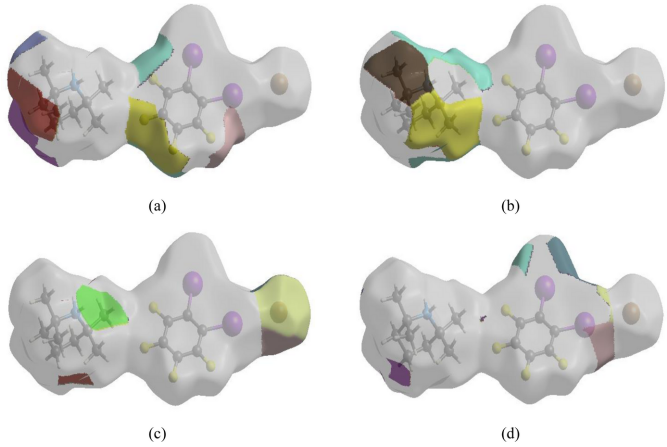

Figure 8
Hirshfeld surface representations of contact patches plotted onto the surface for (*a*) H···F/F···H, (*b*) H···H, (*c*) H···Br/Br···H and (*d*) H···I/I···H interactions.

tips at $d_e + d_i$ = 2.36 Å and $d_e + d_i$ = 3.04 Å, respectively. The F···I/I···F contacts (Fig. 7*f*) make a 7.5% contribution to the HS and have the tips at $d_e + d_i$ = 3.74 Å. The C···I/I···C contacts (Fig. 7*g*) contribute 5.6%, the pair of spikes having tips at $d_e + d_i$ = 3.70 Å. The C···C contacts (Fig. 7*h*) contribute 4.1% to the HS and have a bullet-shaped distribution of points with the tip at $d_e = d_i$ = 1.68 Å. Finally, the F···F (Fig. 7*i*), H···C/C···H (Fig. 7*j*), I···I (Fig. 7*k*), F···Br/Br···F (Fig. 7*l*) and F···C/C···F (not shown) contacts make 1.7%, 1.0%, 0.9%, 0.9% and 0.8% contributions, respectively, to the HS and have very low densities of points.

The nearest neighbour coordination environment of a molecule can be determined from the colour patches on the HS based on how close to other molecules they are. The Hirshfeld surface representations with the fragment patches plotted onto the surface are shown for the H···F/F···H, H···H, H·· Br/Br···H and H···I/I···H interactions in Fig. 8*a*–*d*, respectively.

The Hirshfeld surface analysis confirms the importance of H-atom contacts in establishing the crystal packing. The large number of H···F/F···H, H···H, H···Br/Br···H and H···I/I···H interactions suggest that van der Waals interactions and hydrogen bonding play the major roles in the packing (Hathwar *et al.*, 2015).

5. Database survey

A survey of the Cambridge Structural Database (CSD, Version 5.42, last updated February 2023; Groom *et al.*, 2016) considering both ring motifs indicates that only one molecular structure is closely related to the title compound (I), *viz*. 1-oxy-2,2,6,6-tetramethylpiperidin-4-yl radical benzoate bis-(1,2,3,4-tetrafluoro-5, 6-diiodobenzene), $C_{16}H_{22}NO_3{\cdot}2C_6F_4I_2$ (CSD refcode HISZEQ; Pang *et al.*, 2013). The $C_6F_4I_2$ molecules are essentially identical in their metrical parameters in both structures, while the aliphatic ring system in HISZEQ bears more substituents than in the title compound (I) resulting in small deviations of the overall geometries of the two respective six-membered rings.

Table 3
Experimental details.

Crystal data	
Chemical formula	$C_9H_{20}N^+{\cdot}Br^-{\cdot}C_6F_4I_2$
M_r	624.03
Crystal system, space group	Monoclinic, *C*2/*c*
Temperature (K)	150
a, *b*, *c* (Å)	29.0324 (8), 9.1477 (2), 15.0296 (4)
β (°)	108.533 (1)
V (Å^3)	3784.56 (17)
Z	8
Radiation type	Mo *K*α
μ (mm^{-1})	5.47
Crystal size (mm)	0.25 × 0.21 × 0.19
Data collection	
Diffractometer	Bruker APEXII CCD
Absorption correction	Multi-scan (*SADABS*; Krause *et al.*, 2015)
T_{min}, T_{max}	0.342, 0.423
No. of measured, independent and observed [$I > 2\sigma(I)$] reflections	14152, 3877, 3480
R_{int}	0.022
$(\sin \theta/\lambda)_{max}$ (Å^{-1})	0.627
Refinement	
$R[F^2 > 2\sigma(F^2)]$, $wR(F^2)$, *S*	0.026, 0.069, 1.10
No. of reflections	3877
No. of parameters	220
No. of restraints	2
H-atom treatment	H atoms treated by a mixture of independent and constrained refinement
$\Delta\rho_{max}$, $\Delta\rho_{min}$ (e Å^{-3})	1.50, −0.69

Computer programs: *APEX4* and *SAINT* (Bruker, 2014), *SHELXT2019/1* (Sheldrick, 2015*a*), *SHELXL2019/1* (Sheldrick, 2015*b*) and *SHELXTL* (Sheldrick, 2008).

6. Synthesis and crystallization

TEMPO (10 mmol), 1,2,3,4-tetrafluoro-5,6-diiodobenzene (10 mmol) and CBr_4 (10 mmol) were dissolved in 30 ml of hexane/CH_2Cl_2 (*v*/*v*, 1:1), refluxed for 2 h, and left for slow evaporation. Orange crystals of the product started to form after 2 d at room temperature; they were filtered off and dried in air. Crystals suitable for X-ray analysis were obtained by slow evaporation of a methanol solution. Yield 61% (based on TEMPO), orange powder soluble in methanol, ethanol and DMSO. Analysis calculated for $C_{15}H_{20}BrF_4I_2N$ (M_r = 624.04): C, 28.87; H, 3.23; N, 2.24. Found: C, 28.82; H, 3.20; N, 2.20. ^{1}H NMR (DMSO-d^6), δ: 8.08 (2N–H), 1.73 (2CH_2), 1.65 (CH_2), 1.31 (4CH_3). ^{13}C NMR (DMSO-d^6), 15.6 (CH_2), 26.9 (4CH_3), 34.4 (2CH_2), 57.2 [2C(CH_3)$_2$], 90.5 (2C—I), 148.1 (4C—F).

7. Refinement

Crystal data, data collection and structure refinement details are summarized in Table 3. The N-bound hydrogen atoms were located in a difference-Fourier map, and refined by applying restraints (DFIX). The C-bound H-atom positions were calculated geometrically at distances of 0.99 Å (for CH_2) and 0.98 Å (for CH_3) and refined using a riding model with $U_{iso}(H) = k \times U_{eq}(C)$, where k = 1.2 for CH_2 hydrogen atoms

and k = 1.5 for CH_3 hydrogen atoms. Two reflections were omitted as clear outliers.

Acknowledgements

The authors' contributions are as follows. Conceptualization, AVG, TH and ANB; synthesis, AVG and GZM; X-ray analysis, AVG; writing (review and editing of the manuscript) AVG and TH; funding acquisition, AVG, GZM, KIH and TAJ; supervision, AVG, TH and ANB.

Funding information

This work was supported by the Fundaçao para a Ciencia e a Tecnologia (FCT, Portugal), projects UIDB/00100/2020 (https://doi.org/10.54499/UIDB/00100/2020) and UIDP/00100/2020 (https://doi.org/10.54499/UIDP/00100/2020) of the Centro de Quimica Estrutural and LA/P/0056/2020 (https://doi.org/10.54499/LA/P/0056/2020) of the Institute of Molecular Sciences, as well as Baku State University, Baku Engineering University, Azerbaijan Medical University, Western Caspian University and Khazar University in Azerbaijan. TH is also grateful to the Hacettepe University Scientific Research Project Unit (grant No. 013 D04 602 004).

References

Bruker (2014). *APEX4* and *SAINT*. Bruker AXS Inc., Madison, Wisconsin, USA.

Cavallo, G., Metrangolo, P., Milani, R., Pilati, T., Priimagi, A., Resnati, G. & Terraneo, G. (2016). *Chem. Rev.* **116**, 2478–2601.

Gomila, R. M. & Frontera, A. (2020). *CrystEngComm*, **22**, 7162–7169.

Groom, C. R., Bruno, I. J., Lightfoot, M. P. & Ward, S. C. (2016). *Acta Cryst.* B**72**, 171–179.

Gurbanov, A. V., Kuznetsov, M. L., Mahmudov, K. T., Pombeiro, A. J. L. & Resnati, G. (2020). *Chem. A Eur. J.* **26**, 14833–14837.

Hathwar, V. R., Sist, M., Jørgensen, M. R. V., Mamakhel, A. H., Wang, X., Hoffmann, C. M., Sugimoto, K., Overgaard, J. & Iversen, B. B. (2015). *IUCrJ*, **2**, 563–574.

Hirshfeld, H. L. (1977). *Theor. Chim. Acta*, **44**, 129–138.

Krause, L., Herbst-Irmer, R., Sheldrick, G. M. & Stalke, D. (2015). *J. Appl. Cryst.* **48**, 3–10.

Ma, Z., Mahmudov, K. T., Aliyeva, V. A., Gurbanov, A. V., Guedes da Silva, M. F. C. & Pombeiro, A. J. L. (2021). *Coord. Chem. Rev.* **437**, 213859.

Mahmoudi, G., Dey, L., Chowdhury, H., Bauzá, A., Ghosh, B. K., Kirillov, A. M., Seth, S. K., Gurbanov, A. V. & Frontera, A. (2017*a*). *Inorg. Chim. Acta*, **461**, 192–205.

Mahmoudi, G., Zaręba, J. K., Gurbanov, A. V., Bauzá, A., Zubkov, F. I., Kubicki, M., Stilinović, V., Kinzhybalo, V. & Frontera, A. (2017*b*). *Eur. J. Inorg. Chem.* pp. 4763–4772.

Mahmudov, K. T. & Pombeiro, A. J. L. (2016). *Chem. A Eur. J.* **22**, 16356–16398.

McKinnon, J. J., Jayatilaka, D. & Spackman, M. A. (2007). *Chem. Commun.* pp. 3814–3816.

McKinnon, J. J., Spackman, M. A. & Mitchell, A. S. (2004). *Acta Cryst.* B**60**, 627–668.

Pang, X., Zhao, X. R., Wang, H., Sun, H. L. & Jin, W. J. (2013). *Cryst. Growth Des.* **13**, 3739–3745.

Peuronen, A., Taponen, A. I., Kalenius, E., Lehtonen, A. & Lahtinen, M. (2023). *Angew. Chem. Int. Ed.* **62**, e202215689.

Sheldrick, G. M. (2008). *Acta Cryst.* A**64**, 112–122.

Sheldrick, G. M. (2015*a*). *Acta Cryst.* A**71**, 3–8.

Sheldrick, G. M. (2015*b*). *Acta Cryst.* C**71**, 3–8.

Shixaliyev, N. Q., Gurbanov, A. V., Maharramov, A. M., Mahmudov, K. T., Kopylovich, M. N., Martins, L. M. D. R. S., Muzalevskiy, V. M., Nenajdenko, V. G. & Pombeiro, A. J. L. (2014). *New J. Chem.* **38**, 4807–4815.

Spackman, M. A. & Jayatilaka, D. (2009). *CrystEngComm*, **11**, 19–32.

Spackman, P. R., Turner, M. J., McKinnon, J. J., Wolff, S. K., Grimwood, D. J., Jayatilaka, D. & Spackman, M. A. (2021). *J. Appl. Cryst.* **54**, 1006–1011.

Venkatesan, P., Thamotharan, S., Ilangovan, A., Liang, H. & Sundius, T. (2016). *Spectrochim. Acta A Mol. Biomol. Spectrosc.* **153**, 625–636.

supporting information

Acta Cryst. (2025). E**81**, 53-57 [https://doi.org/10.1107/S2056989024011502]

Crystal structure and Hirshfeld surface analysis of supramolecular aggregate of 2,2,6,6-tetramethylpiperidin-1-ium bromide with 1,2,3,4-tetrafluoro-5,6-diiodobenzene

Atash V. Gurbanov, Tuncer Hökelek, Gunay Z. Mammadova, Khudayar I. Hasanov, Tahir A. Javadzade and Alebel N. Belay

Computing details

(I)

Crystal data

$C_9H_{20}N^+{\cdot}Br^-{\cdot}C_6F_4I_2$
M_r = 624.03
Monoclinic, $C2/c$
a = 29.0324 (8) Å
b = 9.1477 (2) Å
c = 15.0296 (4) Å
β = 108.533 (1)°
V = 3784.56 (17) Å^3
Z = 8
$F(000)$ = 2352
D_x = 2.190 Mg m^{-3}
Mo $K\alpha$ radiation, λ = 0.71073 Å
Cell parameters from 8061 reflections
θ = 2.4–26.4°
μ = 5.47 mm^{-1}
T = 150 K
Prism, orange
0.25 × 0.21 × 0.19 mm

Data collection

Bruker APEXII CCD diffractometer
φ and ω scans
Absorption correction: multi-scan (SADABS; Krause *et al.*, 2015)
T_{min} = 0.342, T_{max} = 0.423
14152 measured reflections
3877 independent reflections
3480 reflections with $I > 2\sigma(I)$
R_{int} = 0.022
θ_{max} = 26.5°, θ_{min} = 2.6°
h = −36→33
k = −11→11
l = −18→18

Refinement

Refinement on F^2
Least-squares matrix: full
$R[F^2 > 2\sigma(F^2)]$ = 0.026
$wR(F^2)$ = 0.069
S = 1.10
3877 reflections
220 parameters
2 restraints
Hydrogen site location: mixed
H atoms treated by a mixture of independent and constrained refinement
$w = 1/[\sigma^2(F_o^2) + (0.0297P)^2 + 23.4044P]$ where $P = (F_o^2 + 2F_c^2)/3$
$(\Delta/\sigma)_{max}$ = 0.003
$\Delta\rho_{max}$ = 1.50 e Å^{-3}
$\Delta\rho_{min}$ = −0.69 e Å^{-3}

Special details

Geometry. All esds (except the esd in the dihedral angle between two l.s. planes) are estimated using the full covariance matrix. The cell esds are taken into account individually in the estimation of esds in distances, angles and torsion angles; correlations between esds in cell parameters are only used when they are defined by crystal symmetry. An approximate (isotropic) treatment of cell esds is used for estimating esds involving l.s. planes.

Fractional atomic coordinates and isotropic or equivalent isotropic displacement parameters (Å²)

	x	*y*	*z*	U_{iso}*/U_{eq}
I1	0.58724 (2)	0.50666 (3)	0.95416 (2)	0.02186 (8)
I2	0.49598 (2)	0.20828 (3)	0.88878 (2)	0.03147 (9)
Br1	0.70229 (2)	0.44644 (4)	1.06238 (3)	0.02025 (10)
F1	0.39660 (9)	0.3559 (3)	0.7874 (2)	0.0358 (6)
F2	0.36882 (9)	0.6336 (3)	0.7483 (2)	0.0385 (7)
F3	0.43515 (10)	0.8520 (3)	0.7953 (2)	0.0402 (7)
F4	0.52828 (10)	0.7943 (3)	0.8811 (2)	0.0350 (6)
N1	0.20902 (12)	0.4228 (4)	0.5387 (2)	0.0168 (7)
C1	0.41559 (15)	0.6043 (5)	0.7915 (3)	0.0273 (10)
C2	0.43063 (15)	0.4616 (5)	0.8126 (3)	0.0251 (9)
C3	0.47865 (15)	0.4272 (5)	0.8587 (3)	0.0223 (8)
C4	0.51296 (14)	0.5399 (5)	0.8839 (3)	0.0208 (8)
C5	0.49698 (15)	0.6813 (5)	0.8607 (3)	0.0247 (9)
C6	0.44896 (16)	0.7134 (5)	0.8155 (3)	0.0285 (10)
C7	0.12586 (15)	0.4790 (5)	0.5367 (3)	0.0258 (9)
H7A	0.095235	0.529016	0.501617	0.031*
H7B	0.117866	0.376129	0.546160	0.031*
C8	0.16011 (14)	0.4814 (4)	0.4774 (3)	0.0203 (8)
C9	0.23227 (14)	0.4809 (4)	0.6381 (3)	0.0200 (8)
C10	0.19400 (15)	0.4749 (5)	0.6869 (3)	0.0241 (9)
H10A	0.207115	0.520952	0.749488	0.029*
H10B	0.186794	0.371383	0.696339	0.029*
C11	0.14695 (15)	0.5518 (5)	0.6321 (3)	0.0270 (9)
H11A	0.123373	0.545906	0.667202	0.032*
H11B	0.153481	0.656302	0.623706	0.032*
C12	0.25235 (15)	0.6339 (5)	0.6354 (3)	0.0261 (9)
H12A	0.273188	0.661239	0.698410	0.039*
H12B	0.225401	0.703502	0.614153	0.039*
H12C	0.271380	0.635554	0.592027	0.039*
C13	0.27448 (14)	0.3797 (5)	0.6841 (3)	0.0249 (9)
H13A	0.289234	0.407421	0.750087	0.037*
H13B	0.298770	0.387430	0.651613	0.037*
H13C	0.262726	0.278711	0.680484	0.037*
C14	0.16547 (16)	0.6325 (5)	0.4403 (3)	0.0290 (10)
H14A	0.191404	0.631076	0.411518	0.043*
H14B	0.173643	0.702913	0.492089	0.043*
H14C	0.134833	0.661096	0.393177	0.043*
C15	0.14272 (15)	0.3773 (5)	0.3950 (3)	0.0245 (9)
H15A	0.165817	0.377765	0.359601	0.037*

H15B	0.110710	0.408459	0.354083	0.037*
H15C	0.140398	0.278296	0.418190	0.037*
H1A	0.2074 (14)	0.330 (2)	0.544 (3)	0.010 (10)*
H1B	0.2309 (15)	0.451 (6)	0.517 (4)	0.040 (15)*

Atomic displacement parameters (Å²)

	U^{11}	U^{22}	U^{33}	U^{12}	U^{13}	U^{23}
I1	0.01724 (13)	0.02663 (16)	0.02143 (14)	−0.00053 (10)	0.00575 (10)	−0.00051 (11)
I2	0.03171 (16)	0.02433 (16)	0.03802 (18)	−0.00134 (12)	0.01060 (13)	0.00187 (12)
Br1	0.01935 (19)	0.0180 (2)	0.0230 (2)	0.00066 (15)	0.00620 (16)	−0.00154 (16)
F1	0.0249 (13)	0.0378 (16)	0.0414 (16)	−0.0114 (12)	0.0058 (12)	0.0024 (13)
F2	0.0188 (12)	0.0524 (18)	0.0406 (16)	0.0086 (12)	0.0040 (11)	0.0072 (14)
F3	0.0398 (15)	0.0286 (15)	0.0507 (18)	0.0130 (12)	0.0121 (14)	0.0063 (14)
F4	0.0361 (14)	0.0235 (14)	0.0428 (16)	−0.0082 (11)	0.0091 (12)	−0.0004 (12)
N1	0.0200 (17)	0.0119 (17)	0.0199 (17)	−0.0013 (13)	0.0083 (14)	0.0011 (13)
C1	0.020 (2)	0.041 (3)	0.022 (2)	0.0036 (18)	0.0077 (17)	0.0035 (19)
C2	0.020 (2)	0.035 (2)	0.021 (2)	−0.0069 (18)	0.0077 (17)	0.0000 (18)
C3	0.025 (2)	0.023 (2)	0.019 (2)	0.0004 (17)	0.0087 (17)	0.0012 (17)
C4	0.0174 (19)	0.026 (2)	0.020 (2)	−0.0006 (16)	0.0067 (16)	−0.0018 (17)
C5	0.025 (2)	0.029 (2)	0.022 (2)	−0.0012 (18)	0.0087 (17)	−0.0022 (18)
C6	0.029 (2)	0.032 (3)	0.026 (2)	0.0066 (19)	0.0115 (19)	0.0037 (19)
C7	0.020 (2)	0.026 (2)	0.030 (2)	0.0017 (17)	0.0072 (18)	0.0010 (19)
C8	0.0186 (19)	0.017 (2)	0.025 (2)	0.0028 (15)	0.0069 (16)	0.0021 (17)
C9	0.0211 (19)	0.020 (2)	0.0185 (19)	−0.0034 (16)	0.0057 (16)	−0.0031 (16)
C10	0.026 (2)	0.026 (2)	0.024 (2)	−0.0024 (17)	0.0127 (18)	−0.0027 (18)
C11	0.025 (2)	0.029 (2)	0.030 (2)	0.0013 (18)	0.0128 (18)	−0.0042 (19)
C12	0.022 (2)	0.024 (2)	0.034 (2)	−0.0055 (17)	0.0112 (18)	−0.0086 (19)
C13	0.021 (2)	0.029 (2)	0.023 (2)	0.0007 (17)	0.0048 (17)	−0.0022 (18)
C14	0.031 (2)	0.020 (2)	0.034 (2)	0.0040 (18)	0.0088 (19)	0.0077 (19)
C15	0.024 (2)	0.023 (2)	0.023 (2)	−0.0002 (17)	0.0030 (17)	0.0022 (17)

Geometric parameters (Å, º)

I1—C4	2.100 (4)	C8—C14	1.517 (6)
I2—C3	2.080 (4)	C9—C10	1.514 (5)
F1—C2	1.348 (5)	C9—C13	1.516 (6)
F2—C1	1.333 (5)	C9—C12	1.522 (6)
F3—C6	1.335 (5)	C10—C11	1.525 (6)
F4—C5	1.346 (5)	C10—H10A	0.9900
N1—C8	1.523 (5)	C10—H10B	0.9900
N1—C9	1.526 (5)	C11—H11A	0.9900
N1—H1A	0.860 (19)	C11—H11B	0.9900
N1—H1B	0.846 (19)	C12—H12A	0.9800
C1—C6	1.357 (7)	C12—H12B	0.9800
C1—C2	1.381 (7)	C12—H12C	0.9800
C2—C3	1.382 (6)	C13—H13A	0.9800
C3—C4	1.399 (6)	C13—H13B	0.9800

C4—C5	1.381 (6)	C13—H13C	0.9800
C5—C6	1.375 (6)	C14—H14A	0.9800
C7—C11	1.522 (6)	C14—H14B	0.9800
C7—C8	1.531 (6)	C14—H14C	0.9800
C7—H7A	0.9900	C15—H15A	0.9800
C7—H7B	0.9900	C15—H15B	0.9800
C8—C15	1.516 (6)	C15—H15C	0.9800

I1···F4	3.138 (3)	C11···H14B	2.83
I1···I2	3.7118 (4)	C12···H11B	2.83
I2···F1	3.111 (3)	C12···H14B	2.67
H1A···Br1^{i}	2.56	C14···H12B	2.72
H13C···Br1^{i}	2.91	C14···H11B	2.90
H1B···Br1^{ii}	2.58 (5)	H1A···H13C	2.22
F1···F2	2.670 (4)	H1A···H15C	2.30
F2···F3	2.709 (4)	H1B···H12C	2.16
F3···F4	2.654 (4)	H1B···H14A	2.32
F2···H12A	2.65	H7B···H15C	2.40
H11A···F3^{iii}	2.63	H11B···H12B	2.19
C12···C14	3.203 (6)	H11B···H14B	2.27
C11···H12B	2.76	H12B···H14B	1.97

C8—N1—C9	120.4 (3)	C10—C9—N1	107.3 (3)
C8—N1—H1A	110 (3)	C13—C9—N1	106.0 (3)
C9—N1—H1A	106 (3)	C12—C9—N1	110.4 (3)
C8—N1—H1B	109 (4)	C9—C10—C11	113.0 (4)
C9—N1—H1B	97 (4)	C9—C10—H10A	109.0
H1A—N1—H1B	114 (5)	C11—C10—H10A	109.0
F2—C1—C6	120.8 (4)	C9—C10—H10B	109.0
F2—C1—C2	120.1 (4)	C11—C10—H10B	109.0
C6—C1—C2	119.2 (4)	H10A—C10—H10B	107.8
F1—C2—C1	117.6 (4)	C7—C11—C10	109.3 (3)
F1—C2—C3	120.7 (4)	C7—C11—H11A	109.8
C1—C2—C3	121.7 (4)	C10—C11—H11A	109.8
C2—C3—C4	119.1 (4)	C7—C11—H11B	109.8
C2—C3—I2	117.7 (3)	C10—C11—H11B	109.8
C4—C3—I2	123.3 (3)	H11A—C11—H11B	108.3
C5—C4—C3	117.9 (4)	C9—C12—H12A	109.5
C5—C4—I1	118.1 (3)	C9—C12—H12B	109.5
C3—C4—I1	124.0 (3)	H12A—C12—H12B	109.5
F4—C5—C6	117.0 (4)	C9—C12—H12C	109.5
F4—C5—C4	120.9 (4)	H12A—C12—H12C	109.5
C6—C5—C4	122.1 (4)	H12B—C12—H12C	109.5
F3—C6—C1	120.0 (4)	C9—C13—H13A	109.5
F3—C6—C5	119.9 (4)	C9—C13—H13B	109.5
C1—C6—C5	120.0 (4)	H13A—C13—H13B	109.5
C11—C7—C8	113.6 (4)	C9—C13—H13C	109.5
C11—C7—H7A	108.8	H13A—C13—H13C	109.5

C8—C7—H7A	108.8	H13B—C13—H13C	109.5
C11—C7—H7B	108.8	C8—C14—H14A	109.5
C8—C7—H7B	108.8	C8—C14—H14B	109.5
H7A—C7—H7B	107.7	H14A—C14—H14B	109.5
C15—C8—C14	108.6 (4)	C8—C14—H14C	109.5
C15—C8—N1	106.1 (3)	H14A—C14—H14C	109.5
C14—C8—N1	111.0 (3)	H14B—C14—H14C	109.5
C15—C8—C7	110.9 (3)	C8—C15—H15A	109.5
C14—C8—C7	112.9 (3)	C8—C15—H15B	109.5
N1—C8—C7	107.2 (3)	H15A—C15—H15B	109.5
C10—C9—C13	111.6 (3)	C8—C15—H15C	109.5
C10—C9—C12	113.1 (3)	H15A—C15—H15C	109.5
C13—C9—C12	108.2 (3)	H15B—C15—H15C	109.5

F2—C1—C2—F1	0.4 (6)	C2—C1—C6—C5	−0.4 (6)
C6—C1—C2—F1	−179.7 (4)	F4—C5—C6—F3	−1.2 (6)
F2—C1—C2—C3	−178.9 (4)	C4—C5—C6—F3	179.3 (4)
C6—C1—C2—C3	1.0 (6)	F4—C5—C6—C1	179.0 (4)
F1—C2—C3—C4	−179.9 (4)	C4—C5—C6—C1	−0.6 (7)
C1—C2—C3—C4	−0.6 (6)	C9—N1—C8—C15	−166.9 (3)
F1—C2—C3—I2	−0.7 (5)	C9—N1—C8—C14	75.4 (4)
C1—C2—C3—I2	178.6 (3)	C9—N1—C8—C7	−48.4 (4)
C2—C3—C4—C5	−0.4 (6)	C11—C7—C8—C15	166.3 (4)
I2—C3—C4—C5	−179.5 (3)	C11—C7—C8—C14	−71.7 (5)
C2—C3—C4—I1	180.0 (3)	C11—C7—C8—N1	50.9 (5)
I2—C3—C4—I1	0.9 (5)	C8—N1—C9—C10	49.8 (4)
C3—C4—C5—F4	−178.6 (4)	C8—N1—C9—C13	169.1 (3)
I1—C4—C5—F4	1.1 (5)	C8—N1—C9—C12	−73.8 (4)
C3—C4—C5—C6	1.0 (6)	C13—C9—C10—C11	−169.0 (4)
I1—C4—C5—C6	−179.4 (3)	C12—C9—C10—C11	68.7 (5)
F2—C1—C6—F3	−0.4 (6)	N1—C9—C10—C11	−53.2 (4)
C2—C1—C6—F3	179.7 (4)	C8—C7—C11—C10	−58.9 (5)
F2—C1—C6—C5	179.5 (4)	C9—C10—C11—C7	60.2 (5)

Symmetry codes: (i) $x-1/2, -y+1/2, z-1/2$; (ii) $-x+1, y, -z+3/2$; (iii) $-x+1/2, y-1/2, -z+3/2$.

Hydrogen-bond geometry (Å, º)

D—H···*A*	*D*—H	H···*A*	*D*···*A*	*D*—H···*A*
N1—H1*A*···Br1^{i}	0.86 (2)	2.55 (2)	3.409 (3)	179 (4)
N1—H1*B*···Br1^{ii}	0.85 (2)	2.58 (3)	3.387 (3)	161 (5)
C13—H13*C*···Br1^{i}	0.98	2.91	3.769 (4)	146

Symmetry codes: (i) $x-1/2, -y+1/2, z-1/2$; (ii) $-x+1, y, -z+3/2$.